

# Elliptic flow of $J/\psi$ at forward rapidity in Pb-Pb collisions at 2.76 TeV with the ALICE experiment

Hongyan Yang (for the ALICE Collaboration)<sup>1</sup>

*SPhN/Trfu, CEA-Saclay, Orme des Merisier, 91191 Gif-sur-Yvette, France*

---

## Abstract

We present the elliptic flow of inclusive  $J/\psi$  measured in the  $\mu^+\mu^-$  channel at forward rapidity ( $2.5 < y < 4.0$ ), down to zero transverse momentum, in Pb-Pb collisions at  $\sqrt{s_{NN}} = 2.76$  TeV with the ALICE muon spectrometer. The  $p_T$  dependence of  $J/\psi$   $v_2$  in non-central (20%-60%) Pb-Pb collisions at  $\sqrt{s_{NN}} = 2.76$  TeV is compared with existing measurements at RHIC and theoretical calculations. The centrality dependence of the  $p_T$ -integrated elliptic flow, as well as the  $p_T$  dependence in several finer centrality classes is presented.

---

## 1. Introduction

Charmonium production in heavy ion collisions has been studied at different energies and with different collision systems, ever since the  $J/\psi$  suppression induced by color screening of its constituent quarks was proposed as a signature of the formation of a quark gluon plasma (QGP) in heavy-ion collisions [1]. The recent measurement of the  $J/\psi$  production in Pb-Pb collisions at forward rapidity performed by ALICE at the LHC [2] clearly showed less suppression compared with SPS and RHIC results [3, 4]. At RHIC energies, the preliminary result from the STAR collaboration showed a  $J/\psi$  elliptic flow in Au-Au collisions at  $\sqrt{s_{NN}} = 200$  GeV [5] consistent with zero within uncertainties in the measured  $p_T$  range (0-10 GeV/c). The measurement of quarkonium elliptic flow is especially promising at the Large Hadron Collider (LHC) where the high energy density of the medium and the large number of  $c\bar{c}$  pairs produced in Pb-Pb collisions is expected to favor the flow development and regeneration scenarios.

## 2. Data analysis and results

The ALICE detector is described in [6]. At forward rapidity ( $2.5 < y < 4.0$ ) the production of quarkonium states is measured in the muon spectrometer down to  $p_T = 0$ . The data sample used for this analysis corresponds to 17 M dimuon unlike sign (MU) triggered Pb-Pb collisions collected in 2011. It corresponds to an integrated luminosity  $L_{int} \approx 70 \mu\text{b}^{-1}$ . The event and muon track selection are the same as described in [7], except for an additional requirement of the event vertex position  $|Z_{vtx}| < 10$  cm to ensure a flat event plane distribution.  $J/\psi$  candidates are formed by combining pairs of opposite-sign (OS) tracks reconstructed in the geometrical acceptance of the muon spectrometer.

---

<sup>1</sup>A list of members of the ALICE Collaboration and acknowledgements can be found at the end of this issue.

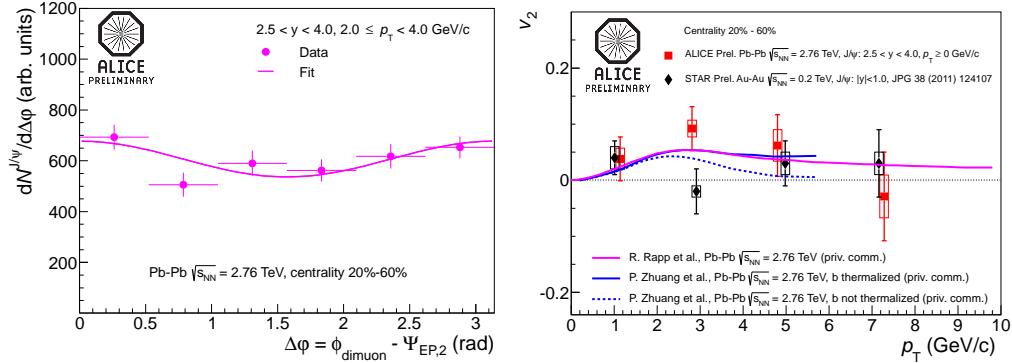


Figure 1: Left:  $v_2$  extraction with the event plane method in which the  $J/\psi$  raw yield is plotted as a function of  $\Delta\varphi$  using a fit to the data with  $dN^{J/\psi}/d\Delta\varphi = A \times (1 + 2v_2^{\text{obs}} \cos 2\Delta\varphi)$ . Right: Inclusive  $J/\psi$   $v_2$  in the centrality bin 20%-60% as a function of  $p_T$ . A comparison to STAR results and to two parton transport model calculations [10, 11] are shown. The vertical bars show the statistical uncertainties, and the boxes indicate the point-to-point uncorrelated systematic uncertainties, which are dominated by the signal extraction.

22 The  $J/\psi$   $v_2$  is measured using event plane based methods [8]. To make a direct comparison  
 23 with lower energy measurements, the inclusive  $J/\psi$   $v_2$  ( $p_T$ ) was calculated in the same centrality  
 24 range 20%-60% as at RHIC [5], as discussed in detail in [9]. The  $v_2$  is extracted by fitting the  $J/\psi$   
 25 raw yield as a function of  $\Delta\varphi = \phi_{\text{dimuon}} - \Psi_{\text{EP},2}$  with  $dN^{J/\psi}/d\Delta\varphi = A \times (1 + 2v_2^{\text{obs}} \cos 2\Delta\varphi)$ , where  
 26  $A$  is a normalization constant (the standard event plane method), as shown in Fig. 1 (left panel).  
 27 At LHC, the event-plane-resolution-corrected  $v_2$  of  $J/\psi$  with  $2 < p_T < 4$  GeV/ $c$  is different from  
 28 the STAR preliminary measurement which is compatible with zero in all the measured  $p_T$  range,  
 29 as shown in Fig. 1 (right panel). Two model calculations based on transport mechanism which  
 30 include a  $J/\psi$  regeneration component from deconfined charm quarks in the medium [10, 11]  
 31 are compared with data. These two models differ mostly in the rate equation controlling the  $J/\psi$   
 32 dissociation and regeneration. In both models about 50% of the produced  $J/\psi$  mesons originate  
 33 from regeneration in QGP in the most central collisions. On one hand, thermalized charm quarks  
 34 in the medium will transfer a significant elliptic flow to regenerated  $J/\psi$ . The maximum  $v_2$  at  
 35  $p_T \approx 2.5$  GeV/ $c$  results from a dominant contribution of regeneration at lower  $p_T$  with respect to  
 36 the initial  $J/\psi$  component. Both models are able to qualitatively describe  $J/\psi$   $v_2(p_T)$  data as both  
 37 were also able to describe the earlier  $R_{\text{AA}}$  measurement [2].

38 Consistent results in the same centrality bin are obtained with an invariant mass fit technique,  
 39 in which we fit the  $v_2 = \langle \cos 2\Delta\varphi \rangle$  vs. invariant mass ( $m_{\mu\mu}$ ) as described in [12]. The method  
 40 involves calculating the  $v_2$  of the OS dimuons as a function of  $m_{\mu\mu}$  and then fitting the resulting  
 41  $v_2(m_{\mu\mu})$  distribution using:  $v_2(m_{\mu\mu}) = v_2^{\text{sig}} \alpha(m_{\mu\mu}) + v_2^{\text{bkg}}(m_{\mu\mu})[1 - \alpha(m_{\mu\mu})]$ , where  $v_2^{\text{sig}}$  is the  $J/\psi$   
 42 elliptic flow and  $v_2^{\text{bkg}}$  is the background flow (parametrized using a second order polynomial  
 43 function in this analysis).  $\alpha(m_{\mu\mu}) = S/(S + B)$  is the ratio of the signal over the sum of the  
 44 signal plus background of the  $m_{\mu\mu}$  distributions.  $\alpha(m_{\mu\mu})$  is extracted from fits to the OS invariant  
 45 mass distribution in each  $p_T$  and centrality class. The OS dimuon invariant mass distribution  
 46 was fitted with a Crystal Ball (CB) function to reproduce the  $J/\psi$  line shape, and either a third  
 47 order polynomial or a variable width gaussian to describe the underlying continuum. The CB  
 48 function connects a Gaussian core with a power-law tail [13] at low mass to account for energy

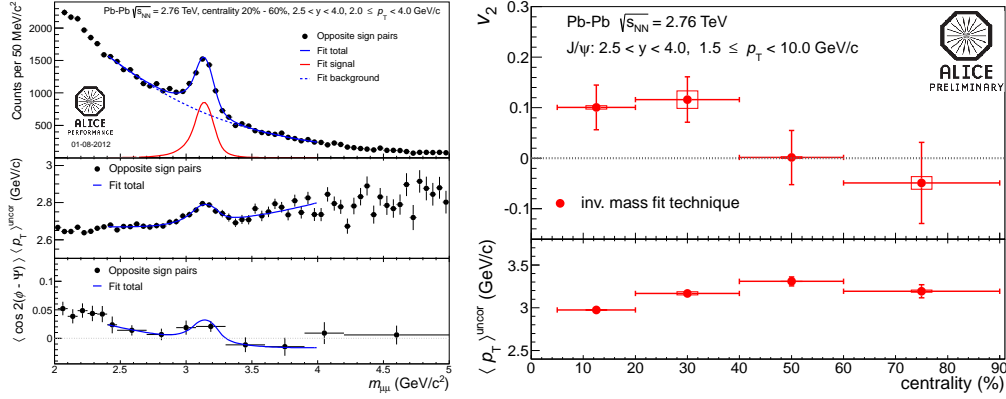


Figure 2: Left:  $\langle p_T \rangle^{\text{uncor}}$  and  $v_2$  extraction with the fit invariant mass technique. Right: Event plane resolution corrected  $J/\psi$   $v_2$  as a function of centrality of  $J/\psi$  with  $p_T \geq 1.5$  GeV/c. The vertical bars show the statistical uncertainties, and the boxes indicate the point-to-point uncorrelated systematic uncertainties, which are dominated by the signal extraction.

49 loss fluctuations and radiative decays. The combination of several CB and underlying continuum  
50 parametrization were tested to assess the signal and the related systematic uncertainties. The  $J/\psi$   
51  $v_2$  in each  $p_T$  and centrality class was determined as the average of the  $v_2^{\text{sig}}$  obtained by fitting  
52  $v_2(m_{\mu\mu})$  with various background shapes, while the corresponding systematic uncertainties were  
53 defined as the *r.m.s.* of these results. A similar method is used to extract the uncorrected average  
54 transverse momentum  $\langle p_T \rangle^{\text{uncor}}$  of the reconstructed  $J/\psi$  in each centrality and  $p_T$  class. Fig. 2  
55 (left panel) shows typical fits of the OS invariant mass distribution (top left), the  $\langle \cos 2(\phi - \Psi_{EP,2}) \rangle$   
56 (bottom left) and  $\langle p_T \rangle^{\text{uncor}}$  (middle left) as a function of  $m_{\mu\mu}$  in the 20%-60% centrality class. The  
57 obtained  $J/\psi$   $\langle p_T \rangle^{\text{uncor}}$  is used to locate the ALICE points when plotted as a function of transverse  
58 momentum.

59 Fig. 2 (top right) shows  $v_2$  for inclusive  $J/\psi$  with  $p_T \geq 1.5$  GeV/c as a function of centrality.  
60 The vertical bars show the statistical uncertainties while the boxes indicate the point-to-point  
61 uncorrelated systematic uncertainties from the signal extraction. The measured  $v_2$  depends on  
62 the  $p_T$  distribution of the reconstructed  $J/\psi$ . Therefore,  $\langle p_T \rangle^{\text{uncor}}$  of the reconstructed  $v_2$  is also  
63 shown in Fig. 2 (bottom right) as a function of centrality. For the two most central bins, 5%-20%  
64 and 20%-40% the inclusive  $J/\psi$   $v_2$  for  $p_T \geq 1.5$  GeV/c are  $0.101 \pm 0.044(\text{stat.}) \pm 0.003(\text{syst.})$   
65 and  $0.116 \pm 0.045(\text{stat.}) \pm 0.017(\text{syst.})$ , respectively. For the two most peripheral bins the  $v_2$  is  
66 consistent with zero within uncertainties. Although there is a small variation with centrality, the  
67  $\langle p_T \rangle^{\text{uncor}}$  stays in the range (3.0, 3.3) GeV/c indicating that the bulk of the reconstructed  $J/\psi$  are  
68 in the same intermediate  $p_T$  range for all centralities. Thus, the observed centrality dependence  
69 of the  $v_2$  for inclusive  $J/\psi$  with  $p_T \geq 1.5$  GeV/c does not result from any bias in the sampled  $p_T$   
70 distributions.

71 Fig. 3 shows the inclusive  $J/\psi$   $v_2(p_T)$ , using the invariant mass fit technique, for central, semi-  
72 central and peripheral Pb-Pb collisions at 2.76 TeV. In the semi-central (20%-40%) case, taking  
73 into account statistical and systematic uncertainties, the combined significance of a non-zero  $v_2$   
74 in  $2 \leq p_T < 6$  GeV/c range is  $3\sigma$ . At lower and higher transverse momentum the inclusive  
75  $J/\psi$   $v_2$  is compatible with zero within uncertainties. In most central (5%-20%) and peripheral  
76 (40%-60%) case, the large uncertainties do not allow any firm conclusion.

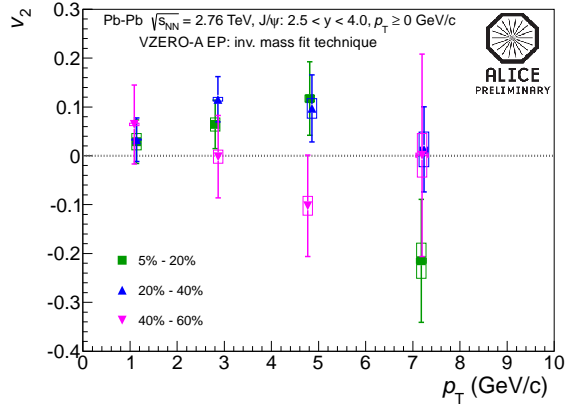


Figure 3:  $J/\psi$   $v_2$  as a function of  $p_T$  in various centrality bins: 5%-20%, 20%-40% and 40%-60%. The vertical bars show the statistical uncertainties, and the boxes indicate the point-to-point uncorrelated systematic uncertainties from the signal extraction.

### 77 3. Summary and conclusion

78 In summary, we reported the ALICE measurement of inclusive  $J/\psi$   $v_2$  at forward rapidity in  
 79 Pb-Pb collisions at  $\sqrt{s_{NN}} = 2.76$  TeV. For non-central (20%-60%) collisions a hint of a non-zero  
 80  $J/\psi$  elliptic flow is observed in the intermediate  $p_T$  range in contrast to the zero  $v_2$  observed at  
 81 RHIC. Indication of a non-zero  $J/\psi$   $v_2$  is also observed in semi-central (20%-40%) collisions at  
 82 intermediate  $p_T$ . The integrated  $v_2$  of  $J/\psi$  with  $p_T > 1.5$  GeV/c in 5%-40% collisions also shows  
 83 a non-zero behavior. These measurements complement our earlier results on  $J/\psi$  suppression,  
 84 where a smaller suppression was seen at low transverse momentum at the LHC compared to  
 85 RHIC [2, 7, 14]. Both results taken together could indicate that a significant fraction of the  
 86 observed  $J/\psi$  are produced from a (re)combination of the initially produced charm quarks. Our  
 87  $J/\psi$  elliptic flow results in Pb-Pb collisions at  $\sqrt{s_{NN}} = 2.76$  TeV are in qualitative agreement with  
 88 transport models that are able to reproduce our  $J/\psi$   $R_{AA}$  measurement.

### 89 References

- 90 [1] T. Matsui and H. Satz, Phys. Lett., B178, p. 416, 1986.  
 91 [2] B. Abelev *et al.* [ALICE Collaboration] Phys. Rev. Lett. 109, 072301, 2012.  
 92 [3] B. Alessandro *et al.*, Eur. Phys. J., C39, p. 335–345, 2005.  
 93 [4] A. Adare *et al.*, Phys. Rev. Lett., 98, p. 232301, 2007; Phys. Rev., C84, p. 054912, 2011.  
 94 [5] Z. Tang [STAR collaboration], J. Phys. G38, 12417, 2011.  
 95 [6] K. Aamodt *et al.*, [ALICE Collaboration], JINST 3, S08002, 2008.  
 96 [7] R. Arnardi, these proceedings.  
 97 [8] A. M. Poskanzer and S. A. Voloshin Phys. Rev. C 58, 1671, 1998.  
 98 [9] L. Massacrier, Hard Probes 2012 proceedings arXiv:1208.5401, and references therein.  
 99 [10] Y.-P. Liu, *et al.*, Phys. Lett. B678, pp. 72–76, 2009 and priv. comm. in 2012.  
 100 [11] X. Zhao and R. Rapp, Nucl. Phys., A 859, pp. 114–125, 2011, R. Rapp these proceedings, and priv. comm. in 2012.  
 101 [12] N. Borghini and J. Ollitrault, Phys. Rev. C70, 064905, 2004, arXiv:nucl-th/0407041 [nucl-th].  
 102 [13] J. E. Gaiser, Ph.D. thesis, Stanford (1982), appendix-F, SLAC-R-255.  
 103 [14] E. Scapparini, these proceedings.